Development of Low Cost, Wireless, Inkjet Printed Microfluidic RF Systems and Devices for Sensing or Tunable Electronics

Chiara Mariotti, *Student Member, IEEE*, Wenjing Su, Benjamin S. Cook, *Member, IEEE*, Luca Roselli, *Senior Member, IEEE*, and Manos M. Tentzeris, *Fellow, IEEE*

***Abstract*— In this paper, a review of recent improvements on inkjet-printed microfluidic-based tunable/sensing RF systems is reported. The devices, such as Radio Frequency IDentification (RFID) passive wireless tags, coplanar patch antennas, bandstop filters, and loop antennas, are all fabricated by combining the inkjet printing technology on photographic paper for metallization and bonding layers, and laser etching for cavities and channels manufacturing. A novelty is also introduced for the loop antennas where the photographic paper is replaced with a polymer based substrate [i.e., (Poly(methyl-methacrylate))], to reduce the substrate losses for the RF part and solve the issue of paper hydrophylia. Along this paper an evolution toward higher working frequencies and higher detecting performance is shown, demonstrating a sensitivity up to $0.5\%/\varepsilon_r$ with at most 6 μL of liquid in the channel.**

***Index Terms*— Microfluidics, sensors, tag, RFID, inkjet printing, tunable electronics.**

I. Introduction

MONITORING and sensing of fluids characteristics and their variations with time and environmental conditions changes, is becoming a relevant function in many areas such as process monitoring, biomedical analysis, water quality measurements and so forth [1]–[3]. For this reason it is important to develop low-cost, environmentally friendly, wireless and energetically autonomous devices that can be connected in distributed networks for liquids sensing. Microfluidics are representing, so far, one of the best solution. Microfluidics, with a simple working principle, allow to analyze, sense and monitor real-time fluids properties with less than 5 μL [4] and sensitivities ranging between $0.2-0.5\%/\varepsilon_r$. However, to really exploit this type of devices, it is fundamental to develop low-cost fabrication processes to replace or combine with traditional techniques. Microfluidic systems are usually fabricated in controlled environments (cleanrooms) with a standard subtractive lithographic process, thus producing chemicals waste and costly products.

Nowadays, several techniques are proposed: laser etched fluidics, craft cut fluidics and wax impregnated capillary action fluidics on paper; all of these methods can be implemented outside of a cleanroom and in a simple way [5]–[7]. However, one issue consists still of integration of the electronic part with the microfluidic, keeping the fabrication cost low, given the fact that to pattern interface and sensing microelectronics onto the chip requires, by now, the use of standard etching technology.

Recently, Cook et al. [4], [8], [9], proposed an innovative technique that combines laser etching of the microfluidic channels and cavities with vertically integrated inkjet printing of circuits on regular photographic paper. In this way, the process is fully out-of-cleanroom and allows for quick and cheap prototyping of integrated monolithic RF electronics. Inkjet printed metallic circuits can be cured and bonded with laser etched microfluidic channels and cavities by printing an adhesive layer and press the microfluidic on top of the RF part. This innovative process is adopted here to demonstrate various microfluidic sensing or tunable RF platforms and devices. In addition, a variant of the process itself is proposed for the first time in this work, with the objective of improving the RF part performance and make the entire device hydrophobic, by replacing the photographic paper with PMMA. Vertically integrated and on-photographic-paper inkjet printing technology has been already proposed and characterized in the past for RF electronics [10]–[14]. Note that, in an industrialization perspective, inkjet printing has the fundamental feature of being compatible with Roll-to-Roll (R2R) technologies thus allowing for the low cost, massive production of these devices [15].

II. Theory of Operation

Electrical properties of fluids exhibit large differences when analyzed at high frequencies. This variability, especially in terms of permittivity (ε_r), conductivity (σ) and losses (tanδ), leads to changes in microwave systems behavior when exposed to the fluid presence (compared to the air). This is the idea on which microfluidic systems work: based on the variation in the RF system response versus frequency it is possible to design

Manuscript received May 31, 2014; revised November 6, 2014; accepted November 11, 2014. Date of publication November 25, 2014; date of current version April 16, 2015. The associate editor coordinating the review of this paper and approving it for publication was Prof. Zheng Cui.

C. Mariotti and L. Roselli are with the Department of Engineering, University of Perugia, Perugia 06100, Italy (e-mail: chiaramariotti23@gmail.com; luca.roselli@unipg.it).

W. Su, B. S. Cook, and M. M. Tentzeris are with the School of Electrical and Computer Engineering, Georgia Institute of Technology, Atlanta, GA 30332 USA (e-mail: wsu36@gatech.edu; bcook40@mail.gatech.edu; etentze@ece.gatech.edu).

Color versions of one or more of the figures in this paper are available online at http://ieeexplore.ieee.org.

Digital Object Identifier 10.1109/JSEN.2014.2374874

TABLE I
ELECTRICAL PROPERTIES OF USED FLUIDS AT 300 K [15]–[19]

Fluid	Real (ε')	Imaginary (ε'')
Air	1	0
Water	64-73	8
Hexanol	3	2.5
Glycerol	4	0.4
Ethanol	6	7.1

sensors and tunable electronic devices. Moreover, some liquids exhibit a change in electrical properties with temperature variation: this feature can also be exploited in order to realize temperature, microfluidic-based tunable electronics or sensors. The design procedure consists of studying and choosing a certain geometry and a working frequency, then the RF circuit is designed, considering an empty channel, and optimized in terms of tunable range and sensitivity by simulating the structure varying the permittivity of the fluid into the channel. Finally, the experiments are fitted with the CAD response. In Table I, the electrical properties of the fluids used to test the proposed devices, are reported.

III. FABRICATION PROCESS

The fabrication process is a large part of the novelty introduced by the microfluidic-based devices proposed in this work. The reason is that it allows for the realization of low-cost microfluidic-based RF systems by combining vertically integrated inkjet printing technology with laser methods. This approach has been already adopted in [4], [8], [9], and [20] demonstrating the possibility of rapid prototyping of low-cost, eco-compatible and innovative RF microfluidic antennas, RFID systems, varactors and filters.

Note that at the end of this paper an improvement of this method is also illustrated and proved, showing very good results obtained with microfluidic-based tunable/sensing loop antennas.

A. Materials and Platforms Used

The substrate used for the microfluidic is a 1/16-in-thick cast acrylic sheet (Poly(methyl-methacrylate)) (PMMA) (Mcmaster-Carr, Atlanta, GA, USA) into which cavities and channels are etched; the electrical circuit is instead inkjet printed on a 220-μm-thick Kodak Premium Photo Paper (Office Depot). The conductive layer is realized by means of ANP nanoparticle based silver [21]. In order to bond the PMMA on paper a SU-8 polymer solution (MicroChem, Newton, MA, USA) is used, while the RF connectors and RFID chips attaching is obtained by applying the Circuit Works 60 Minute Cure Conducitve Epoxy (Chemtronix, Kennesaw, GA, USA).

Channels and cavities are etched on PMMA by using an Epilog Legend 36EXT laser machine, while the printing platform for the RF part is the Dimatix DMP-2800. The photo paper and the PMMA sheets are bonded using an inkjet printed SU-8 layer which has the double role of gluing and insulation layer.

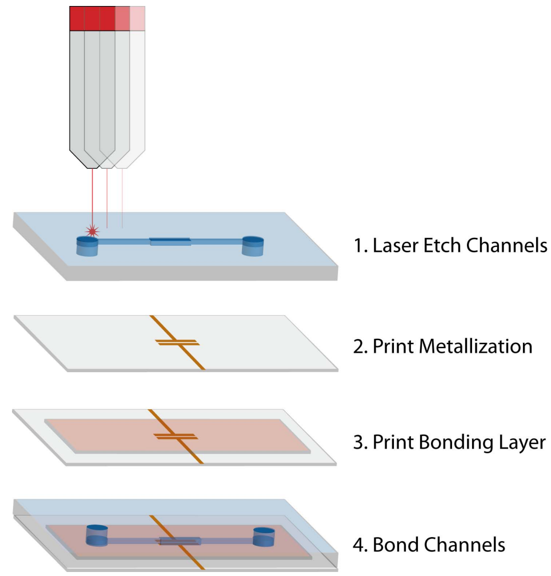

Fig. 1. Illustration of the microfluidic devices fabrication process. After [4].

B. Process Description Step-by-Step

The process is illustrated step-by-step in Fig. 1. Firstly channels and cavities are laser etched on the PMMA substrate; subsequently the designed circuit is inkjet printed on photographic paper and baked into the oven at 120°C for one hour. Flash curing for 2 to 5 minutes at 180°C can be used to improve the metalization conductivity. At this point, the two substrates, are ready for the bonding step: 3 layers of SU-8 ink are printed onto the circuit on paper and then the etched PMMA is bonded on top of it exploiting the adhesive properties of the SU-8. To finalize the bonding, a force of 10 N/cm^2 is applied on PMMA, while the whole structure is placed on a hotplate at 100°C.

Once the bonding procedure is completed microfluidic connectors can be glued on the PMMA holes in order to allow fluid injection, while the RF connectors can be soldered by using conductive-adhesive which curing is done at room temperature. Finally, the device is ready for testing.

IV. MICROFLUIDIC RFID PLATFORM

A microfluidic, wireless and passive RFID sensing tag fabricated with the process described in Sec. III is reported here as a first demonstration of the technology. The idea is to fabricate a microfluidic tunable/sensing antenna to be connected to a RFID tag IC that, when interrogated by the reader, responds at a certain frequency based on the fluid pumped into the channel.

The proposed RFID tag is designed to operate with the Alien Technologies, Higgs 3EPC Gen-2 RFID chip, in the readable range of the Voyantic Tagformance reader which works at $800 - 1000$ MHz. As the resonant frequency of the tag will only shift downwards when a fluid is introduced into the channel, the operating frequency of the tag with an empty channel has been optimized for 1000 MHz. The design tool used for this work is the CST frequency domain solver. A photograph of the fabricated circuit is shown in Fig. 2 while the channel is filled with water. In this picture it is

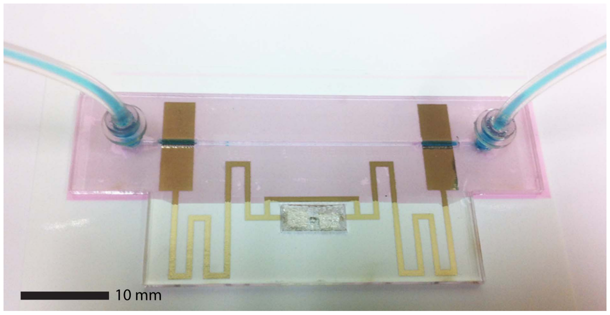

Fig. 2. Fabricated RFID-based microfluidic tag with inkjet printed antenna, laser-etched channel and inkjet printed SU-8 bonding layer. After [4].

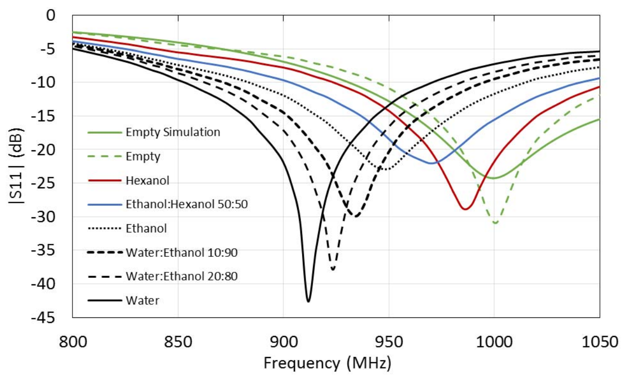

Fig. 3. Measured and simulated return loss of the microfluidic RFID tag. After [4].

possible to notice the RFID tag that is connected to the printed antenna on paper. In order to verify the functionality of the antenna a cabled measurement of the s-parameters is taken by using a Rhode and Schwartz ZVA-8 VNA. The results are then re-normalized to the RFID chip impedance. From Fig. 3 it can be seen that simulated and measured return loss agree when the channel is empty while a downward shift in the resonant frequency is experienced when the channel is filled with hexanol, ethanol, water or a mixture of them in various ratios as reported in the graph legend. This behavior is expected since the fluids have a higher permittivity compared to the air. Once verified that the antenna is working as expected and its resonant frequency can be tuned by pumping a fluid into the channel, a wireless measurement has been performed to see the functionality of the complete platform. The graphs in Fig. 4 show the tag activation power when interrogated with a signal at 1000 MHz and 900 MHz. The measurement setup is composed by the tag placed 50 cm away from the reader antenna of the Tagformance that interrogates it in the frequency range of $800 - 1000$ MHz. The data obtained by the Tagformance are related to the power needed to activate the tag and the reflected power and phase versus frequency.

From the returned results it can be seen that the activation power slightly decreases with the higher permittivity fluids which is due to the improving matching between the antenna and the chip impedance. Moreover, it is noticed that comparing the wireless measurements with the cabled ones, the tag exhibits lower shifts and this is reasonable considering the variation in chip impedance over frequency. This also causes a decreased sensitivity.

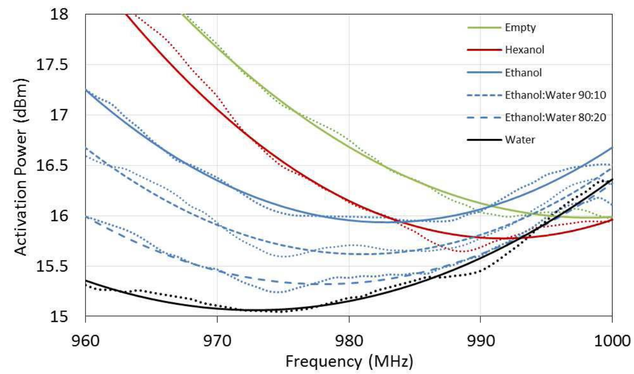

(a)

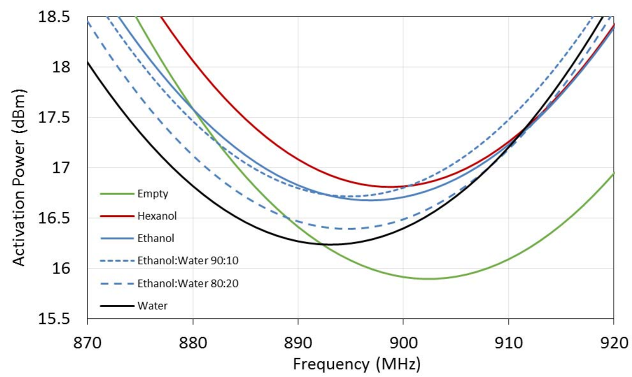

(b)

Fig. 4. Curves fit backscatter data of a microfluidic tag with resonant frequency of (a) 1 GHz and (b) 900 MHz. After [4].

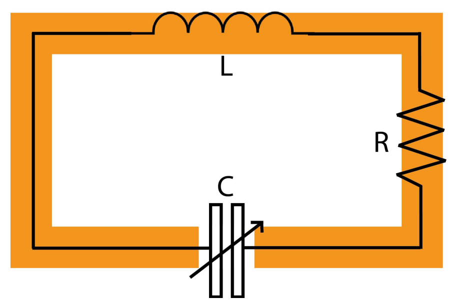

Fig. 5. Series R-L-C model of the bandstop filter. After [8].

V. Microfluidic Bandstop Filter

In this section a first evolution towards higher working frequencies and sensitivities is reported by demonstrating a Split-Ring-Resonator (SRR) based bandstop filter that exhibits a sensitivity of $0.4\%/\varepsilon_r$ utilizing only 6 μL of fluid in the channel. The device is fabricated with the same process. The proposed circuit is a tunable bandstop filter usually adopted as meta-surface unit-cell. The equivalent circuit of the SRR is reported in Fig. 5: a series R-L-C model is used, where R represents parasitic losses, L is the loop inductance and C is the gap capacitance. The resonant frequency can be determined with Eq. 1 and its tuning is obtained with the fluid flowing into the channel on top of the SRR gap. This gap is in fact modeled as a capacitance and, as a consequence, any fluid in the channel changes the permittivity of the capacitance insulation material thus causing a higher value of capacitance

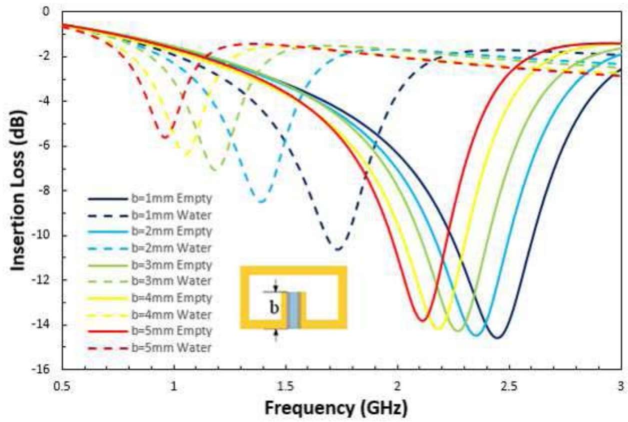

Fig. 6. Parametric analysis of the gap size. After [8].

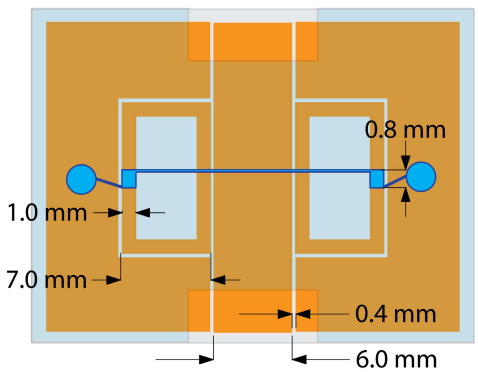

(a)

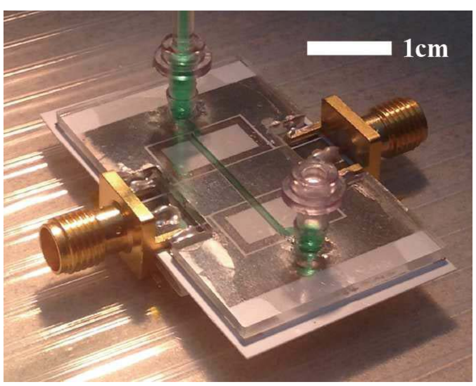

(b)

Fig. 7. (a) Design of the bandstop filter unit cell with dimensions and (b) photograph of the fabricated prototype. After [8].

(compared to an empty channel) and a downwards resonant frequency shift.

The selected geometry has been chosen mainly because it is simple to inkjet printing manufacturing. The dimensions are calculated to make the structure resonate at 2.4 GHz when the channel is empty. The gap size effect on the performance has been studied with a parametric simulation and then a gap of 1 mm by 0.8 mm is adopted in order to maximize the tunable range of the device. The parametric study is reported in Fig. 6.

$$f = \frac{1}{(2\pi\sqrt{LC})} \quad (1)$$

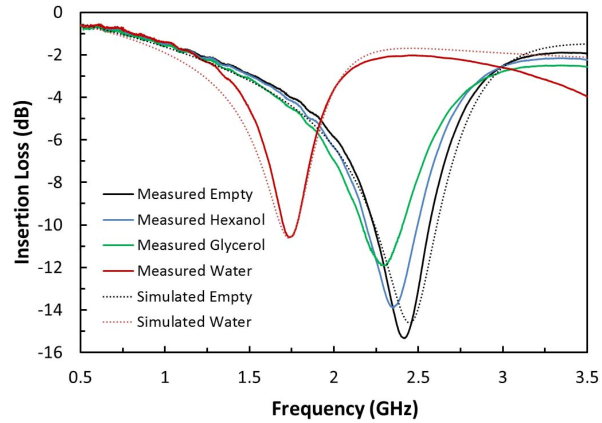

(a)

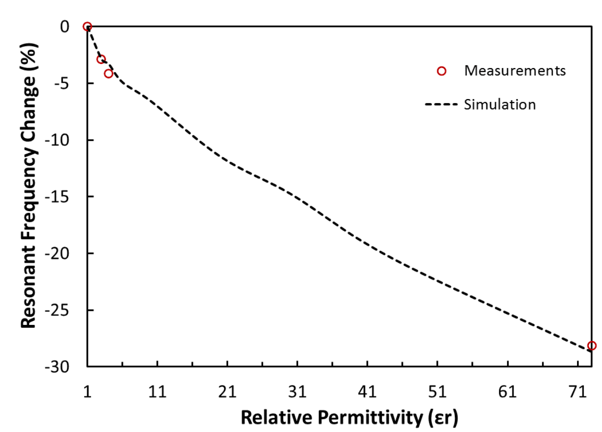

(b)

Fig. 8. Measured and simulated results for the bandstop filter: (a) insertion loss for different fluids and (b) resonant frequency shift (in percentage) due to different fluids in the channel. After [8].

Figure 7.a is an illustration of the bandstop filter unit-cell design with the dimensions reported on it, while in Fig. 7.b a picture of the realized and tested prototype is shown. When the channel is empty the resonant frequency is about 2.4 GHz while adding hexanol, glycerol or water it goes down to 1.6 GHz. The experienced sensitivity is $0.4\%/\varepsilon_r$, thus demonstrating an improvement compared to what reported in literature [19].

It is worth noticing that the 3 dB filter bandwidths from empty condition to filled with hexanol, glycerol and water are 8.3%, 8.5%, 13% and 12.6% respectively.

The curves for the measured and simulated results are in Fig. 8: a good agreement between CAD results and experiments for those cases accounted for, namely: air hexanol, glycerol (first three points left top corner of the graph in Fig. 8.b) and water (bottom right corner). A tunable range of about 650 MHz is experienced when the channel is filled with water (that is a very high permittivity fluid) Fig.8.a.

A. Temperature Stability Measurement

An important analysis for RF devices is related to the test of their temperature stability. This feature is even more important

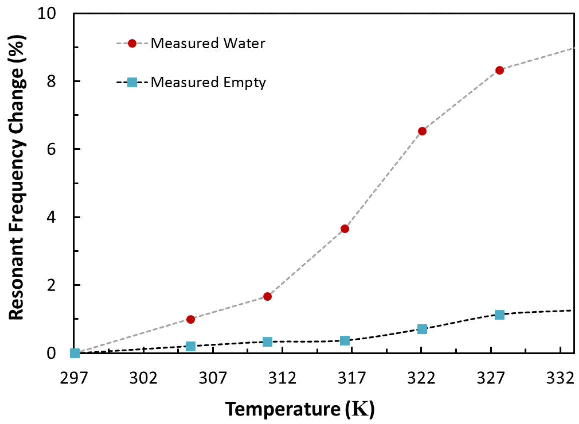

Fig. 9. Resonant frequency change (in percentage) due to temperature change.

when the device is a fluid-tunable or sensing system considering that fluids are usually characterized by big variations in permittivity over temperature. The test is performed by a calibration step in which the channel is filled with air and the temperature is raised from room temperature (i.e. 297 K) to 332 K. The measured insertion loss is stable showing a variation within 1% and it goes back to the initial curve when the temperature is lowered to room temperature. This small change can be easily considered when calibrating the final results in a practical system. As already stated, many fluids experience a change in the relative permittivity when the temperature is changed; water, for instance, is known to perform a decrease of 21% in relative permittivity from 297 K to 332 K as reported in [22]. Therefore the experiment is repeated with the channel filled with water and it can be seen from Fig. 9 that the resonant frequency shift is of about 9% due to the raised temperature and thus due to the decreased permittivity. It is worth underlining that combining what reported in literature for water permittivity change over temperature (i.e. 21%) with the measured device sensitivity, a 8.4% change is expected, that is very close to the 9% obtained from measurements. Again, the device returns back to its original behavior when restoring the room temperature condition.

VI. Microfluidic Coplanar Fed Patch Antenna

Following the RFID platform and the SRR bandstop filter a third microfluidic fluid-tunable/sensing device realized with the same process is proposed. In this section a microfluidic coplanar fed patch antenna the resonant frequency of which is 3.8 GHz, when the channel is empty, and 3.3 GHz, when it is filled with water, is described.

The design, depicted in Fig. 10, is characterized by the Coplanar Patch Antenna (CPA), that can be described as a patch antenna surrounded by the ground plane on the same substrate side. The behavior, in term of electric field analysis, is similar to that of a microstrip patch antenna; the phase of the electrical field is the same on the top and bottom slots, while a 180 degrees of change is performed on the left and right slots demonstrating that the CPAs have two radiating edges and two non-radiating edges [23]. The microfluidic channel is placed on top of the front radiation edge, as shown in Fig. 10,

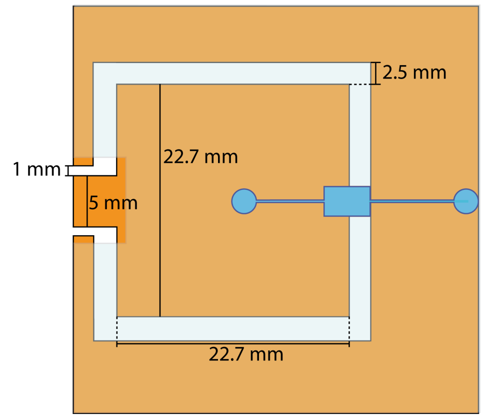

(a)

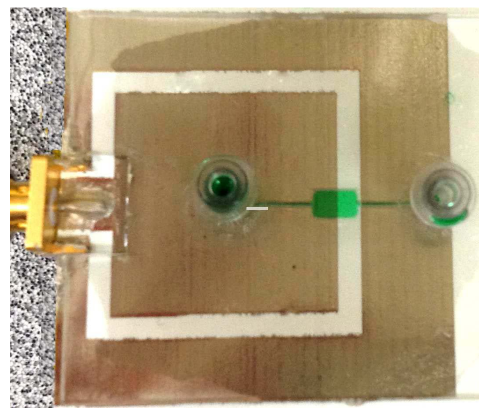

(b)

Fig. 10. Coplanar patch antenna with water filled microfluidic channel: (a) design with dimensions and (b) photograph of the prototype. After [9].

where the channel is filled with water. The CPA operating frequency is tuned by pumping fluids into the channel thus modifying the relative permittivity on top of the radiating edge. The simulated and measured S-parameters and radiation patterns are reported in Fig. 11, showing a tuning range of 500 MHz for permittivity values between 1 (empty) and 63.8 (water). The radiation pattern experiences, as expected, two peaks for the E-plane and a circular shape for the H-plane. Note that the radiation pattern remains nearly the same over the tunable range.

VII. Microfluidic-Based Tunable Loop Antenna

The fabrication process described and adopted for the RF circuits proposed in the previous sections is demonstrated and well consolidated at lab-level, however a variant of it is now introduced.

Photographic paper, used as a substrate for metalization, has high dielectric losses and hydrophilic properties, thus limiting the endurance and functionalities of these sensors and tunable systems. For these reasons, the challenge with the new process is to introduce a substrate able to reduce or overlap these limits: PMMA is a good candidate considering that it is low-cost, hydrophobic, with lower dielectric losses than paper and compatible with inkjet printing of both conductive and bonding/insulation layers.

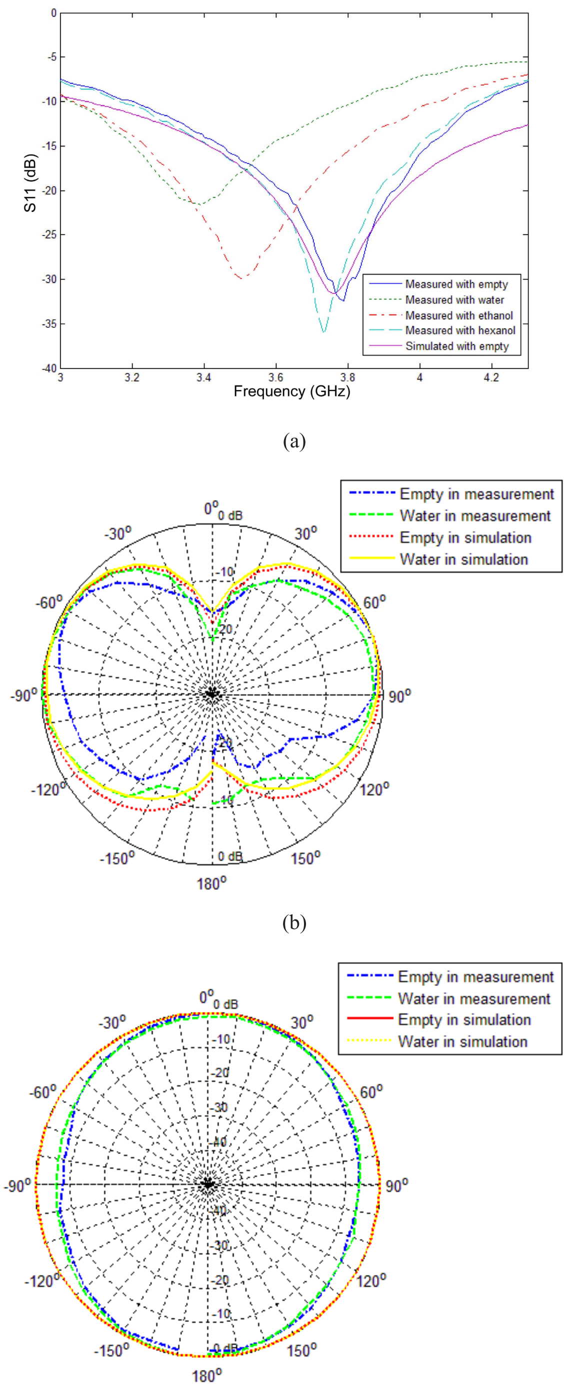

(a)

(b)

(c)

Fig. 11. CPA measurement results: (a) S-parameters when the channel is empty or filled with water, ethanol or hexanol, (b) E-plane radiation pattern and (c) H-plane radiation pattern. After [9].

In order to demonstrate the feasibility of PMMA-based method a loop antenna has been designed, simulated and then fabricated and tested.

The fabrication process is depicted in Fig. 12. The EMD5730 SunTronic Jettable silver ink is printed on a 1.5 mm thick PMMA sheet. The sintering procedure is different from the usual baking into the oven because the PMMA cannot endure the high temperature normally used to cure the silver ink, thus in this case the epilogue laser is employed at 24 W.

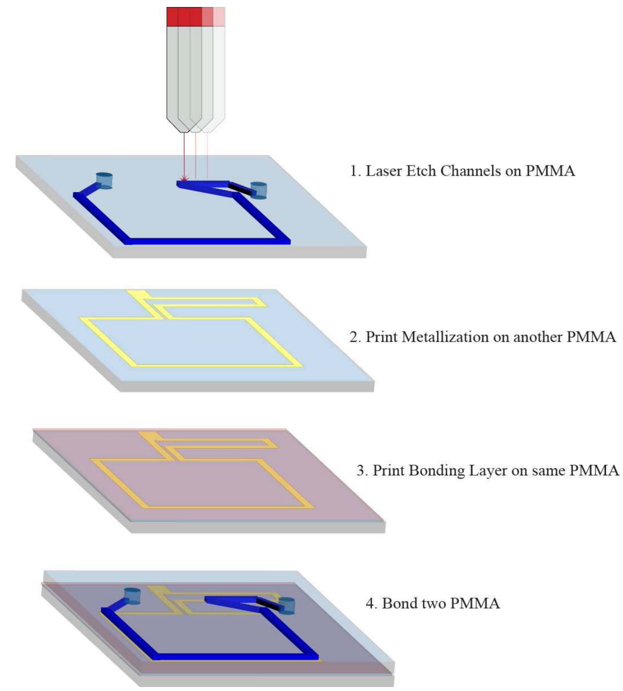

Fig. 12. Novel fabrication process: the substrate for metalization printing is PMMA instead of paper.

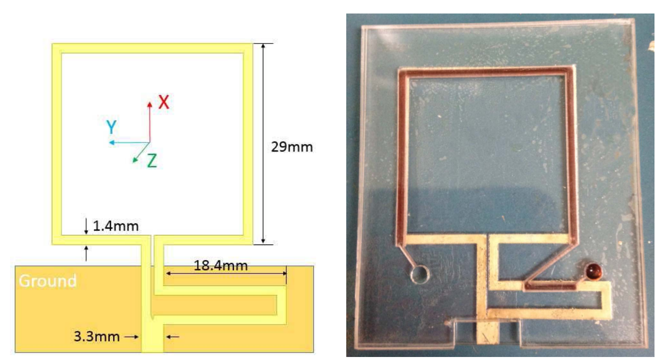

(a) (b)

Fig. 13. Loop antenna: (a) design with dimensions and (b) photography of the fabricated device.

The microfluidic channels and cavities are etched as usual on a 1.5 mm thick PMMA sheet. Then 3 layers of SU-8 are deposited on the RF part as adhesive film and it is exposed to 300 mJ/cm^2. The two PMMA sheets are bonded applying a force of 10 N/cm^2 and heating the whole structure at 100°C for 5 minutes.

A. Loop Antenna Design

Loop antenna is well-known as a magnetic dipole. A square loop, the edge of which is 29 mm long, has been designed, as illustrated in Fig. 13.a. The microfluidic channel is placed on top of the loop and the permittivity of the fluid pumped in it, effectively controls the electrical length of the loop. In this way, the resonant frequency of the loop is tuned. In order to feed the antenna with a coaxial cable, a balun transformer is introduced. The balun is composed by a power divider and two microstrip lines with 180 degree of phase difference.

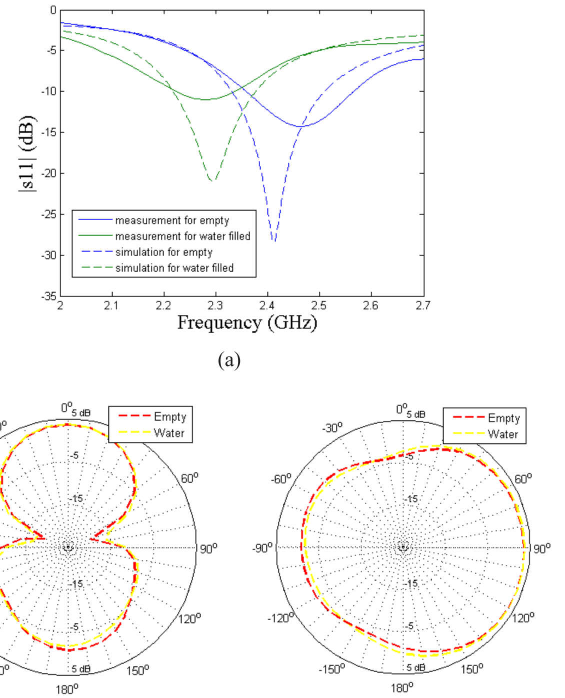

Fig. 14. Loop antenna results: (a) S-parameters and simulated radiation pattern (b) E-plane and (c) H-plane. The tested conditions are with the channel empty or filled with water.

Note that the channel is placed also on top of the transformer lines in order to calibrate the frequency shift determined by the microfluidic and guarantee the equality between the antenna and the balun operating frequency. In addition, with this technique, the same efficiency over all the reconfigurable frequency range, is maintained.

B. Results

The loop antenna has been simulated with ANSYS HFSS, fabricated and then tested in the two cases in which the channel is empty or filled with water. The antenna return loss and radiation pattern results are reported in Fig. 14.

A frequency shift from 2.45 GHz (empty channel) to 2.28 GHz (channel with water) is experienced in the s-parameters test; a good matching with simulations is also demonstrated, even though the input matching is worse than expected and this might be due to the balun design, which has to be better optimized.

VIII. Conclusion

The feasibility of RF microfluidic-based sensing and tunable devices, fabricated by combining inkjet printing technologies and laser etching techniques, is proved. A sensitivity up to $0.5\%/\varepsilon_r$ is achieved with less than $6\,\mu$L of fluid pumped into the channel. The fabrication process is described with its variant in which photographic paper is replaced by PMMA in order to improve the circuit performance and durability, being the PMMA lower lossy and hydrophobic. Devices such as RFID tags, coplanar patch antennas, bandstop filters and loop antennas, working at frequencies ranging from 900 MHz to 3.3 GHz, are reported, demonstrating the importance of combining microfluidics with low-cost and simple fabrication processes and opening the door to cheap and rapid prototyping of platforms for bio-monitoring and real-time fluids analysis.

References

[1] D. B. Weibel and G. M. Whitesides, "Applications of microfluidics in chemical biology," *Current Opinion Chem. Biol.*, vol. 10, no. 6, pp. 584–591, 2006.

[2] N. Blow, "Microfluidics: In search of a killer application," *Nature Methods*, vol. 4, no. 8, pp. 666–670, 2007. [Online]. Available: http://web.stanford.edu/group/foundry/about/articles/nature_meth07.pdf

[3] *Microfluidics and Microfluidic Devices: A Review*. [Online]. Available: http://www.elveflow.com/microfluidic-reviews-and-tutorials/microfluidics-and-microfluidic-devices-a-review, accessed 2014.

[4] B. S. Cook, J. R. Cooper, and M. M. Tentzeris, "An inkjet-printed microfluidic RFID-enabled platform for wireless lab-on-chip applications," *IEEE Trans. Microw. Theory Techn.*, vol. 61, no. 12, pp. 4714–4723, Dec. 2013.

[5] A. W. Martinez, S. T. Phillips, B. J. Wiley, M. Gupta, and G. M. Whitesides, "FLASH: A rapid method for prototyping paper-based microfluidic devices," *Lab Chip*, vol. 8, no. 12, pp. 2146–2150, 2008.

[6] H. Klank, J. P. Kutter, and O. Geschke, "CO_2-laser micromachining and back-end processing for rapid production of PMMA-based microfluidic systems," *Lab Chip*, vol. 2, no. 4, pp. 242–246, 2002.

[7] P. K. Yuen and V. N. Goral, "Low-cost rapid prototyping of flexible microfluidic devices using a desktop digital craft cutter," *Lab Chip*, vol. 10, no. 3, pp. 384–387, 2010.

[8] W. Su, C. Mariotti, B. S. Cook, S. Lim, L. Roselli, and M. M. Tentzeris, "A metamaterial-inspired temperature stable inkjet-printed microfluidic tunable bandstop filter," *Eur. Microw. Week (EuMW) Rome*, Oct. 2014, pp. 5–10.

[9] W. Su, C. Mariotti, B. S. Cook, L. Roselli, and M. M. Tentzeris, "A novel inkjet-printed microfluidic tunable coplanar patch antenna," in *Proc. IEEE Int. Symp. Antennas Propag.*, Jul. 2014, pp. 858–859.

[10] S. H. Ko, J. Chung, H. Pan, C. P. Grigoropoulos, and D. Poulikakos, "Fabrication of multilayer passive and active electric components on polymer using inkjet printing and low temperature laser processing," *Sens. Actuators A, Phys.*, vol. 134, no. 1, pp. 161–168, 2007.

[11] M. Jung *et al.*, "All-printed and roll-to-roll-printable 13.56-MHz-operated 1-bit RF tag on plastic foils," *IEEE Trans. Electron. Devices*, vol. 57, no. 3, pp. 571–580, Mar. 2010.

[12] A. Rida, L. Yang, R. Vyas, and M. M. Tentzeris, "Conductive inkjet-printed antennas on flexible low-cost paper-based substrates for RFID and WSN applications," *IEEE Antennas Propag. Mag.*, vol. 51, no. 3, pp. 13–23, Jun. 2009.

[13] B. J. Kang, C. K. Lee, and J. H. Oh, "All-inkjet-printed electrical components and circuit fabrication on a plastic substrate," *Microelectron. Eng.*, vol. 97, pp. 251–254, Sep. 2012. [Online]. Available: http://www.sciencedirect.com/science/article/pii/S0167931712001311

[14] B. S. Cook *et al.*, "Inkjet-printed, vertically-integrated, high-performance inductors and transformers on flexible LCP substrate," in *Proc. IEEE MTT-S Int. Microw. Symp. (IMS)*, Jun. 2014, pp. 1–4.

[15] A. Tidar *et al.*, "Microwave dielectric relaxation study of 1-hexanol with 1-propenol mixture by using time domain reflectometry at 300 K," in *Proc. Appl. Electromagn. Conf. (AEMC)*, 2009, pp. 1–4.

[16] R. R. Nigmatullin, M. M. A.-G. Jafar, N. Shinyashiki, S. Sudo, and S. Yagihara, "Recognition of a new permittivity function for glycerol by the use of the eigen-coordinates method," *J. Non-Crystalline Solids*, vol. 305, nos. 1–3, pp. 96–111, 2002. [Online]. Available: http://www.sciencedirect.com/science/article/pii/S0022309302011250

[17] K. Shibata, "Measurement of complex permittivity for liquid materials using the open-ended cut-off waveguide reflection method," in *Proc. China-Jpn. Joint Microw. Conf. (CJMW)*, 2011, pp. 1–4.

[18] A. E. Lipton, M. K. Griffin, and A. G. Ling, "Microwave transfer model differences in remote sensing of cloud liquid water at low temperatures," *IEEE Trans. Geosci. Remote Sens.*, vol. 37, no. 1, pp. 620–623, Jan. 1999.

[19] T. Chretiennot, D. Dubuc, and K. Grenier, "A microwave and microfluidic planar resonator for efficient and accurate complex permittivity characterization of aqueous solutions," *IEEE Trans. Microw. Theory Techn.*, vol. 61, no. 2, pp. 972–978, Feb. 2013.

[20] B. S. Cook, J. R. Cooper, S. Kim, and M. M. Tentzeris, "A novel inkjet-printed passive microfluidic RFID-based sensing platform," in *Proc. IMS*, Jun. 2013, pp. 1–3.

[21] *ANP Nano-Silver Ink for Inkjet Printing*, [Online]. Available: http://anapro.com/eng/product/silver_inkjet_ink.html, accessed 2014.

[22] A. Catenaccio, Y. Daruich, and C. Magallanes, "Temperature dependence of the permittivity of water," *Chem. Phys. Lett.*, vol. 367, nos. 5–6, pp. 669–671, 2003. [Online]. Available: http://www.sciencedirect.com/science/article/pii/S0009261402017359

[23] K. Li, C. H. Cheng, T. Matsui, and M. Izutsu, "Coplanar patch antennas: Principle, simulation and experiment," in *Proc. IEEE Antennas Propag. Soc. Int. Symp.*, vol. 3, Jul. 2001, pp. 402–405.

Chiara Mariotti was born in Perugia, Italy, in 1987. She received the Laurea (*magna cum laude*) degree in electronic and telecommunication engineering from the University of Perugia, Perugia, in 2011. In Spring 2012, she was with the ATHENA Research Group, Georgia Institute of Technology, Atlanta, GA, USA, for six months, working on eco-compatible indoor localization systems and other devices fabricated by means of inkjet printing technology on regular photographic paper. She is currently pursuing the Ph.D. degree at the High Frequency Electronics Laboratory, University of Perugia, with a focus on green technologies for passive and energetically autonomous RFID tags. In 2013, she was with the ATHENA Research Group to work on vertically integrated inkjet-printed systems and devices such as passives and microfluidics sensors on several substrates (i.e., LCP, silicon, and paper). Recently, she spent five weeks at the Institute of Telecommunication, University of Aveiro, Aveiro, Portugal, to work on devices for wireless power transfer and RF energy harvesting, fabricated on unusual materials, such as cork and wood and to be embedded into floors, walls, and ceilings.

Wenjing Su was born in Hunan, China, in 1991. She received the B.S. degree in electrical engineering from the Beijing Institute of Technology, Beijing, China, in 2013. She is currently pursuing the Ph.D. degree in electrical and computer engineering at the Georgia Institute of Technology, Atlanta, GA, USA. In Fall 2013, she joined the ATHENA Research Group and worked as a Research Assistant. Her research focuses on inkjet-printed passive sensors and reconfigurable electronics.

Benjamin S. Cook (S'12) received the B.Sc. degree from the Rose-Hulman Institute of Technology, Terre Haute, IN, USA, in 2010, the M.A.Sc. degree from the King Abdullah University of Science and Technology, Thuwal, Saudi Arabia, in 2011, and the Ph.D. degree from the Georgia Institute of Technology, Atlanta, GA, USA, in 2014, all in electrical engineering.

He has authored or co-authored over 25 peer-reviewed publications. His research focuses are in inkjet process design for vertically integrated millimeter-wave devices, system-on-paper applications, green electroncs, microelectromechanical systems device fabrication, RF energy harvesting, and passive wireless sensors. He was the recipient of the Outstanding Senior Electrical and Computer Engineering Student of the Year Award from the Rose-Hulman Institute of Technology, the King Abdullah University of Science and Technology (KAUST) Fellowship Award in 2010, and the KAUST Provost Award in 2011. During his Ph.D. work, he received the IEEE Antennas and Propagation Society Doctoral Research Award and the Intel Doctoral Fellowship for his work in vertically integrated inkjet fabrication for millimeter-wave applications.

Luca Roselli (M'92–SM'01) was born in Florence, Italy, in 1962. He received the Laurea degree in electronic engineering from the University of Florence, Florence, in 1988, where he worked on SAW devices from 1988 to 1991. In 1991, he joined the University of Perugia, Perugia, Italy, where he is currently an Associate Professor and has taught several classes on electronic devices, microwave electronics, HF electronic components, and applied electronics. Since 2000, he has coordinated the research activity of the High Frequency Electronics Laboratory, University of Perugia. In 2000, he founded the spinoff company Wireless Solutions Srl, operating in the field of microwave electronic systems, which he cooperated as a Consultant until it joined the new company ART srl in 2008. From 2008 to 2012, he was the Director of the Technical and Scientific Committee, ART srl and a member of the Board of Directors.

He founded a second spinoff company Digital Electronic Solutions Srl in 2005. He was the Chairman of the Seventh Computational Electromagnetic in Time Domain Workshop in 2007 and the First IEEE WPTC Conference in 2013.

He is currently a member of the list of experts of the Italian Ministry of Research and University, a member of several IEEE Technical Committees [MTT-24 RFID Technologies (Past Chair), MTT-25 RF Nanotechnolgies, and MTT-26 Wireless Power Transfer), a member of the Sub Committee 32 RFID Technologies of International Microwave Symposium (Past Chair), a member of the European Research Council Panel PE7, a member of the Advisory Committee of IEEE WPTC Conference, involved in the Boards of several international conferences (RWCOM, RFID-TA, EuCAP, and MAREW), and a reviewer for many international conferences and reviews [the PROCEEDINGS OF THE IEEE, the IEEE Microwave Theory and Techniques Society, the IEEE MICROWAVE AND WIRELESS COMPONENTS LETTERS, *Advances in Chemical Engineering and Science Journal*, *Radioengineering Journal*, Hindawi Publishing Corporation, *Organic Electronics* (Elsevier), and *Nanoscience and Nanotechnology Letters* (ASP)].

His research interests mainly focus on the design of high-frequency electronic circuits and systems, including the development of numerical methods for electronic circuit analysis with a special attention to RFID-NFC systems, new materials (including organic and recyclable ones), and far-field wireless power transfer.

In these fields, he has published over 220 contributions to international reviews and peer-reviewed conferences, the interest in which is testified by an HF index of 20 (Scholar font) and over 1350 citations.

Manos M. Tentzeris (S'89–M'92–SM'03–F'10) received the Diploma (*magna cum laude*) degree in electrical and computer engineering from the National Technical University of Athens, Athens, Greece, and the M.S. and Ph.D. degrees in electrical engineering and computer science from the University of Michigan, Ann Arbor, MI, USA.

He is currently a Professor with the School of Electrical and Computer Engineering, Georgia Institute of Technology (Georgia Tech), Atlanta, GA, USA. He has authored or co-authored over 420 papers in refereed journals and conference proceedings, five books, and 19 book chapters. He has helped develop academic programs in Highly Integrated/Multilayer Packaging for RF and Wireless Applications using ceramic and organic flexible materials, paper-based RFIDs and sensors, biosensors, wearable electronics, inkjet-printed electronics, green electronics and power scavenging, nanotechnology applications in RF, microwave microelectromechanical systems, SOP-integrated (UWB, multiband, millimeter-wave, and conformal) antennas and adaptive numerical electromagnetics Technical Interest Group, and served as the Associate Director for RFID/Sensors Research with the Georgia Electronic Design Center, Atlanta, from 2006 to 2010, and the Associate Director for RF Research and the RF Alliance Leader of the NSF-Packaging Research Center at Georgia Tech from 2003 to 2006.